# Compressibility of BiCu 2 PO 6 : Polymorphism against S = 1 / 2 Magnetic Spin Ladders

Marie Colmont, C. Darie, Alexander Tsirlin, Anton Jesche, Claire Colin, Olivier Mentré

# Compressibility of $BiCu_2PO_6$: polymorphism against S=1/2 magnetic spin ladders

Marie Colmont[†] Céline Darie,[†] Alexander A. Tsirlin,*[‖] Anton Jesche, [‖] Claire Colin, [†] and Olivier Mentré*[†]

[†]Univ. Lille, CNRS, Centrale Lille, ENSCL, Univ. Artois, UMR 8181 - UCCS - Unité de Catalyse et Chimie du Solide, F-59000 Lille, France

[†]Université Grenoble Alpes et CNRS, Institut NEEL, F-38042 Grenoble, France

[‖] Experimental Physics VI, Center for Correlations and Magnetism, Institute of Physics, University of Augsburg, 86135 Augsburg, Germany

*Supporting information*

**ABSTRACT:** $BiCu_2PO_6$ is an unique example of S=1/2 ladder where the magnetic exchanges are mainly confined in 1D-$_\infty[BiCu_2O_2]^{3+}$ cationic ribbons, although the existence of shortest Cu-Cu separation between them. Its original magnetic topology gives the most representative example of frustrated quantum ladder to investigate the complex physics behind. Herein, we report the synthesis and characterization of one high-pressure polymorph. In this new phase, the preservation of 1D- $_\infty[BiCu_2O_2]^{3+}$ units somewhat restacked leads to the preservation of its gapped magnetic ground state and ladder topology. The comparison between both compounds highlight a scare thermodynamic conjuncture, where both the stable ambient pressure (AP) and the metastable high pressure (HP) forms display the same equilibrium volume and superposed volume dependence of the energy , leading to a 1st order AP → HP transition undetected by DTA.

$BiCu_2PO_6$ (BCPO) is a S=1/2 ladder system with a unique magnetic behaviour due to frustration of spin ladders along their legs [1-2]. In this compound, there is a strong discrepancy between the structural ladders and the magnetic ones in that sense that the shortest Cu-Cu distance of 2.89 Å along the structural rungs, leads to only a weak magnetic coupling J3, following cancellation of ferromagnetic and antiferromagnetic terms. On the opposite, long-range interactions (J4), mediated by oxygen and bismuth bridges with Cu-Cu distances exceeding 5 Å, turn out to be strong and reinstate the ladder-like interaction topology, but now with spin ladders formed between the structural ladder-like units (see Figure 1). This would be a mere oddity, unless further long-range interactions had come into play. Such interactions, labelled J2 hereinafter, connect next nearest neighbour (NNN) along the legs (Figure 1c). They naturally compete with nearest-neighbour (NN) interactions J1 and render $BiCu_2PO_6$ a unique representative of copper-based quantum magnets that triggers long-standing interest of the physics community [3-8].

On the physics side, the main interest in BCPO stems from the fact that this compound lacks long-range magnetic order and instead exhibits an unusual spin gap, i.e., a gap $\Delta/k_B$ =32-45 K separating the first excited state from the ground state. Unlike in the conventional spin-dimers systems, two excitations branches are formed owing to the giant anisotropic spin interactions [9-11]. Closing the gap in applied magnetic fields leads to a cascade of magnetic transitions into a plethora of novel magnetic states, including soliton lattices, whereas excitations over the gap serve as a model case for quasiparticle-continuum level repulsion, as probed in inelastic neutron scattering experiments [12-13]. In addition recent evidences of the suppression of the BCPO thermal conductivity at low temperature increasing the magnetic field due to strong spin-phonon coupling opens the perspectives of strong magnetoelectric coupling [10,14].

From the structural viewpoint, these peculiar properties result from a specific ladder topology induced by the aptitude of both $Cu^{2+}$ and $Bi^{3+}$ ions to occupy the corners of oxo-centered tetrahedra arranged in edge-sharing units, i.e. the double $_\infty[BiCu_2O_2]^{3+}$ zig-zag chains in BCPO shown in the figure 1 (see ref. [15] for a review), which naturally create the $Cu^{2+}$ zig zag chains. Here, due to the strongly covalent O-Cu and O-Bi bonds compared to the external Bi/Cu --- $OPO_3$ bonds, the magnetic units form the rigid framework of the crystal structure. High pressure/high temperature (HP/HT) treatments have been applied in order to probe the possibility of re-organization between them in a denser polymorph. In this paper, the ambient-pressure $BiCu_2PO_6$ (AP-BCPO) and its high-pressure variant (HP-BCPO) will be presented and juxtaposed.

Single phase HP-BCPO material was achieved by the HP/HT transformation of AP-$BiCu_2PO_6$ at 5GPa/800°C. The AP-$BiCu_2PO_6$ polycrystalline precursor was preliminary prepared at 800°C from a stoichiometric mixture of $Bi_2O_3$, CuO, and $(NH_4)H_2PO_4$ as reported in [3,16]. It was then packed into a platinum capsule, jointly pressed and heated using a belt system apparatus. Details about the synthesis are given in Supplementary informations, S1. After releasing the pressure, HP-BCPO is stable and its XRD pattern shows drastic changes compared to AP-BCPO. It was fully indexed in the orthorhombic unit cell a= 12.26003(8) Å, b= 5.21763(4) Å and c= 7.27982(5) Å with respect to the Pnma symmetry, reminiscent of the $BiCu_2AsO_6$ (BCAO) crystal lattice [17]. The Rietveld refinement using the BCAO starting model leads to final agreement factors $R_{Bragg}$ = 4.36% and $R_f$ = 2.67% using constrained P-O distances due to the slightly "out-of range" P-O bonds. A more accurate model for oxygen positions was obtained after DFT relaxation of the refined structure fixing the experimental lattice parameters, see S2 by comparison to AP-BCPO. The main interatomic distances and angles in these units for the two BCPO forms are compared in the table 1. In this table, the labels J1 to J4 respects the nomenclature used in ref [3], as shown in figure 1. Density-functional band-structure calculations performed on the GGA+U level ($U_d$=9.5 eV and $J_d$=1eV) lead to the exchange couplings Ji compared in table 1 for both the AP and HP forms.

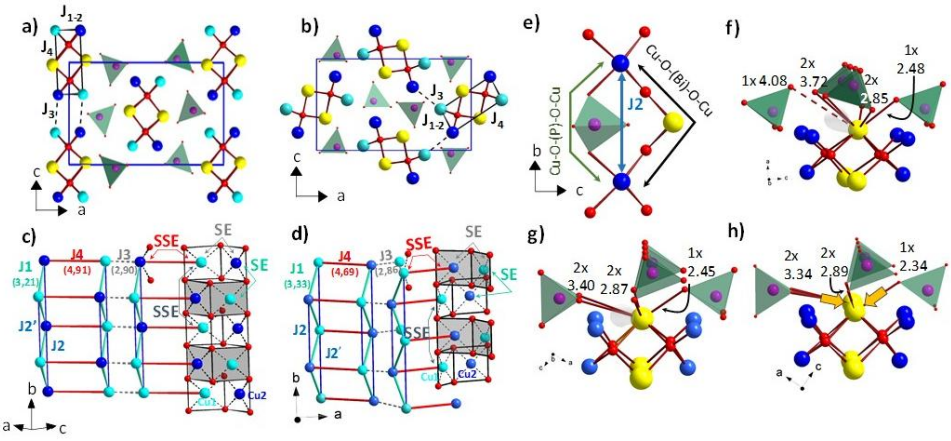


**Figure 1:** Projection along the b-axis of the $BiCu_2PO_6$ crystal structure with evidence of polycationic ribbons surrounded by $XO_4$ groups with (a) X= P and (b) X= As. The $Cu^{2+}$ zigzag ladders are formed between the two ribbons, as shown by the dotted lines. The ribbons and ladders stretched along the b,-axis with the distance labelling scheme with different J-J coupling schemes for (c) X= P and (d) X= As. e) two paths of the J2 exchange. The interaction between the $XO_4$ groups and oxo-centered units in f) AP-BCPO; g) HP-BCPO; and h) $BiCu_2AsO_6$.

**Table 1:** Geometrical parameters associated with the SE and SSE paths in the AP and HP (ICSD# 434030)polymorphs of $BiCu_2PO_6$.

| Magnetism : exchange and path | | AP | HP | Geometric features | AP | HP |
|---|---|---|---|---|---|---|
| J1/Kb (K) | SE (legs) Cu-O-Cu | 114 | 181 | Cu1-Cu2 (Å)<br>Cu1-O1-Cu2 (°) | 3.21<br>112.2 | 3.32<br>119.6 |
| J2/Kb (K) | SSE (NNN-legs) Cu-O-(P)-O-Cu and Cu-O-(Bi)-O-Cu | 68 | 95 | Cu1-Cu1 (Å)<br>O2-O2 (Å)<br>∠Cu1-O2-O2-Cu1 (°)<br>O1-O1 (Å)<br>∠Cu1-O1-O1-Cu1 (°) | 5.17<br>2.56<br>0<br>2.55<br>0 | 5.22<br>2.56<br>0<br>2.60<br>0 |
| J2'/Kb (K) | SSE (NNN-legs) Cu-O-(P)-O-Cu and Cu-O-(Bi)-O-Cu | 117 | 108 | Cu2-Cu2 (Å)<br>O2-O2 (Å)<br>∠Cu-O2-O2-Cu (°)<br>O1-O1 (Å)<br>∠Cu-O1-O1-Cu (°) | 5.17<br>2.56<br>0<br>2.63<br>0 | 5.22<br>2.56<br>0<br>2.61<br>0 |
| J3/Kb (K) | SE (inter-ladders) Cu-O-Cu | 30 | -30 | Cu1-Cu2 (Å)<br>Cu1-O2-Cu2 (°) | 2.90<br>92.0 | 2.86<br>92.1 |
| J4/Kb (K) | SSE (rungs) Cu-O-(Bi)-O-Cu | 103 | 84 | Cu1-Cu2 (Å)<br>O2-O2 (Å)<br>∠Cu1-O2-O2-Cu2 (°) | 4.91<br>2.75<br>0.8 | 4.66<br>2.75<br>10.1 |

At this stage, several main features should be noted: i) the ratio between the cell volumes of AP-BCPO and HP-BCPO is 1.02, i.e. 474.56 Å3/465.67 Å3, confirms the HP transformation into a more dense crystal packing. ii) the conservation of the nearly unchanged $_\infty[BiCu_2O_2]^{3+}$ oxo-centered units suggests that basic features of the magnetic lattice, along with its exotic magnetic ground state, should be preserved, see figure 1 c,d. In the AP-form, $_\infty[BiCu_2O_2]^{3+}$ magnetic ladders grow parallel, whereas in HP-BCPO the ladders are rotated by ca. 100° and arranged in a crisscrossed pattern. iii) Similar to AP-BCPO, the coupling J3 between the magnetic units (i.e., within the structural ladders) is expected to be relatively weak because of the nearly orthogonal orbital overlaps (i.e. Cu-O-Cu = 92.1°). On the other hand, the rung super-super-exchange coupling J4 can be substantial, because the ∠Cu-O…O-Cu dihedral angle is small (i.e., ~10.1°) and the O…O contact distances (2.749 Å) are within the Van der Waals distance [18]. This reinstates remarkably similar spin ladder topologies between AP-BCPO and HP-BCPO, although the main structural context is drastically modified.

Experimentally, the absence of a magnetic ordering transition and the sharp decrease of the magnetic susceptibility $\chi(T)$ below $T_{max}$ = 43K indicate a spin gap, similar to AP-BCPO. Our data collected at several applied fields between 0.1 and 7T show a significant, field-dependent upturn below 10K typical of defect paramagnetism. Due to the presence of a minor ferromagnetic impurity not detected by XRD, we have focused on the 1T data after checking that the shape of $\chi(T)$ is field-independent above 10K. We have used several approaches to the magnetic modelling, ranging from an analytical approximation to the exact diagonalization, to elucidate this complex case.

First, we fitted the susceptibility using the high-temperature series expansion for a simple S= 1/2 ladder $\chi_L$(g, J1, J4), see details in S3. In view of the sizable inter-ladder coupling J3 the expression was modified taking into account the inter-ladder interactions on a mean-field level via an effective temperature $\theta_{int}$. The Curie-type impurity term and the $\chi 0$ temperature-independent term were included as well:

$$\chi = \chi_0 + x_{imp}C/(T-\theta_{imp}) + (1-x_{imp})\,\chi_L/[1-(\theta_{int}\,\chi_L/C)] \quad (1)$$

with C = 0.375 $cm^3$ K $mol^{-1}$ , $\theta_{int}$ = z S(S+1) $J_3/3K_b$ and z=4 surrounding ladders via $J_3$. After fixing g=2.2 and $J_1/J_4$ = 1.8 (from DFT calculations below) we found antiferromagnetic $J1/K_b$= 88.8(3)K (i.e. $J_4/K_b$ =49K) and ferromagnetic $J_3/K_b$ = -4.85(2) K, $\chi_0$=2.2.$10^{-4}$ $cm^3$ $mol^{-1}$ $x_{imp}$= 1.75(2)% and $\theta_{imp}$ = -2.44(6) K giving a rough approximation of the J's involved and the deduced gap of 22 K (see S3).

The shortcomings of this approach are the absence of the second-neighbour couplings J2, J2' and, consequently, the neglected effect on the gap, which can be remedied by a simple fit using the relation:

$$\chi = \chi_0 + x_{imp}C/(T-\theta_{imp}) + A\exp(-\Delta/T)/\sqrt{T} \quad (2)$$

in the low-temperature part. This leads to the accurate Δ = 27.9(1)K value very similar to the gap of 32K in the AP-form [2]. Including J2 and J2' in a full temperature range is more difficult, because magnetic frustration is introduced, and the analytical expression for $\chi_L$ no longer holds. Nevertheless, we can use the exact result for a single spin ladder with J1, J2, J2', and J4, but neglect J3. This leads to a very good fit above 100 K (g=2.15 and the approximation J1=200K, J2=J2'=J1/2 and J4 =140K) and compares favourably with the exchange couplings obtained from DFT, see S3. On the other hand, the low-temperature part is not reproduced, because the interladder coupling J3 is crucial for the size of the spin gap. The model without J3 overestimates the gap and, therefore, shifts the susceptibility maximum toward higher temperatures. All fits are presented in Figure 2a.

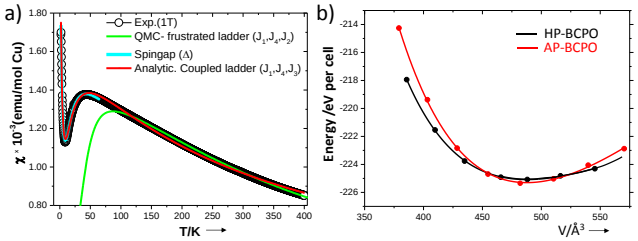


**Figure 2:** a) Experimental magnetic susceptibility under 1T and its fits using models described in the text. b) Fit of the energy-vs-volume curves for the HP and AP polymorphs.

The exchange couplings in BCPO are far from trivial. It is striking that most exchanges are calculated to be stronger in the HP form despite the longer Cu-Cu distances. This confirms the primordial role of the SE and SSE mechanisms in these compounds. For example, the leg coupling J1 is strongly enhanced due to the increase in the Cu-O-Cu bridging angle. On the other hand, J4 is reduced in the HP polymorph, because the bigger dihedral angle of 10.1° (see iii) above and table 1) renders the super-superexchange pathway more curved and, consequently, less efficient [18]. Finally, the sharp difference between J2 and J2' in the AP-form, despite the equal Cu-Cu distances of 5.17 Å, was discussed in the previous literature, but remains largely unclear. The HP-form gives new insights here for better rationalization of the hierarchy of magnetic exchanges. By comparing the structural parameters of the AP and HP polymorphs, we find a clear correlation between the size of J2(J2') and the O-O distances within the Cu-O-(P)-O-Cu and Cu-O-(Bi)-O-Cu paths, see figure 1e,f,g,h. The sizes of J2 and J2' are scaled by the length of the O-O contact, which are differentiated at the bismuth side.

We now study the compressibility and thermodynamic stability of the two forms. Although HP-BCPO is denser than AP-BCPO, most of the cation-cation and cation-anion bond distances involved in the structural and spin ladders are slightly longer in the HP-form, which is rather unusual and may be due to the sterically active $Bi^{3+}$ lone pair that is external to these units. We computed total energies of the AP- and HP-polymorphs as a function of volume and fitted the resulting E(V) dependencies using the Birch-Murnaghan equation of state (EOS), see figure 2b.[19]. Dertails are given in S3. The results highlight a very unusual behavior giving $E_0$ (eV/cell), $V_0$ (Å$^3$), $B_0$ (GPa), $B_{0'}$ = -225.302, 487.7, 82.6, 5.96 for the AP-form and -225.082, 487.8, 53.3, 8.37 for the HP-form. DFT systematically overestimates equilibrium cell volumes $V_0$, but provides a surprising result of nearly the same $V_0$ in both structures despite the drastic structural reorganization. The equilibrium energy $E_0$ (i.e. the energy at the minimum) for the HP structure is 0.22 eV/cell (i.e. 55 meV/f.u. ~ 5.33 kJ/mol) higher than that of the AP structure, which confirms metastable nature of the HP-form at ambient conditions. More intriguingly, both the bulk modulus $B_0$ (inversely proportional to the compressibility) and its pressure derivative B'= $dB_0/dP$ (which scales the pressure effect of the bulk modulus) reveal higher compressibility of the HP-form. The HP-BCPO is thus as soft as $Bi_4Ge_3O_{12}$ ($B_0$ = 48 GPa, B' = 9), although formed under pressure. [20], [21] To the best of our knowledge, this counter-intuitive hardness hierarchy $AP_{hard}$>$HP_{soft}$ has not been previously seen in compounds of lone-pair cations, where pressure-induced phase transition typically produce a harder structure, e.g. $PbCrO_3$ I ($B_0$=59 GPa) → II ($B_0$= 187 GPa) [22] with its giant volume collapse, or α-$BiB_3O_6$ I($B_0$= 38GPa) → II($B_0$=114 GPa) [23, 24]. In contrast, less compressible (i.e. high bulk modulus) structures are generally stable in a broad pressure range, e.g. $Bi_2Al_4O_9$ ($B_0$= 122 GPa), $Bi_2Mn_4O_{10}$ ($B_0$= 138 GPa) [25].

The high compressibility of the HP-form compared to the AP one can be explained by structural arguments, keeping in mind its analogy with $BiCu_2AsO_6$ compound. It is well established that the compressibility of $Bi^{3+}$ compounds is driven by the flexibility of the $BiO_x$ polyhedra, including the stereo-activity of the lone electron pair [26]. The four $PO_4$ groups in the vicinity of $Bi^{3+}$ involve the $BiO_4^{+6}$ main polyhedron in the AP-form, in contrast to the $BiO_4^{+5}$ polyhedron in the HP-form, where the four short Bi-O bonds point toward the magnetic units, see figure 1f,g.

Dealing with the long Bi-O bonds, the oxygen packing shows O---O bonds in the order of magnitude of the Van der Waals distances, which involves a less dense (i.e. more compressible) HP form due to its lower Bi coordination. In addition, the comparison between the BCAO and the HP-BCPO structures shows significant shrinkage of Bi-O bonds in the former by up to 4.5% as shown by arrows on the figure 1,h. This shrinkage compensates for the presence of longer As-O bonds compared to P-O bonds, thus leaving a room for the large compression of HP-BCPO with its smaller $PO_4$ groups, in agreement with our EOS fits.

In fine, HP-BCPO is metastable at ambient pressure and has been quenched upon cooling inside our high-pressure setup. A harder HP polytype may be expected at higher pressures, similar to assumptions given for the $Bi_{12}SiO_{20}$ sillenite ($B_0$=63.4) with no detected transition up to ca. 17 GPa. [26].

HP-BCPO transforms abruptly back into the AP-form at ca. 690°C as shown by high temperature XRD that reveals a 1st order transition, see figure 3a. However, the splitting of XRD peaks suggests a distribution of compositions after quenching to RT, i.e., a phase separation into two AP-related compounds in the approximatively 1:1 ratio with the lattice parameters a=11.781, b=5.171, c=7.789 (very close to the reported AP form) and a=11.757, b=5.163, c=7.664 (contracted cell), Figure 3b. It is reminiscent of the off-stoichiometry that could occur by $Bi^{3+}$ for $Cu^{2+}$ partial substitution, see the related series with the mixed $Bi^{3+}/M^{2+}$ sites (15) and/or $Bi^{3+}$ inclusions within the $Cu^{2+}$ chains, see the $Bi_{2+x}Cu_{1-2x}O_4$ case (27). At high temperature, this phase separation results in two distinct melting points ($Tm_1$ =874°C, $Tm_2$ =888 °C) being lower than those of the AP-form ($Tm_{AP}$ =903 °C). The melting is congruent and the single recrystallization peak is detected on cooling at T =833°C. Together they show similar melting/recrystallization hysteresis (ΔT = ca. 60°C) as in the

stoichiometric compound when similar thermal treatments (heating rate = 5°C/min) are used, Figure 3b.

In conclusion, we have prepared at 5GPa, 800°C a new high-pressure (HP) polymorph of the well-known $BiCu_2PO_6$ compound, fascinating due to its unique spin-gap ground state that results from frustrated S=1/2 ladders. In the HP-form, the magnetic layers are preserved but twisted, such that a novel spin-gap ground state is reached with the reinforced leg couplings (J1) and plethora of potential specificities with regards to the intensive properties previously explored in the ambient-pressure (AP) parent compound. The structural relationship between the AP and HP polytypes validates the role of the covalent oxocentered $_{\infty}[BiCu_2O_2]^{3+}$ units

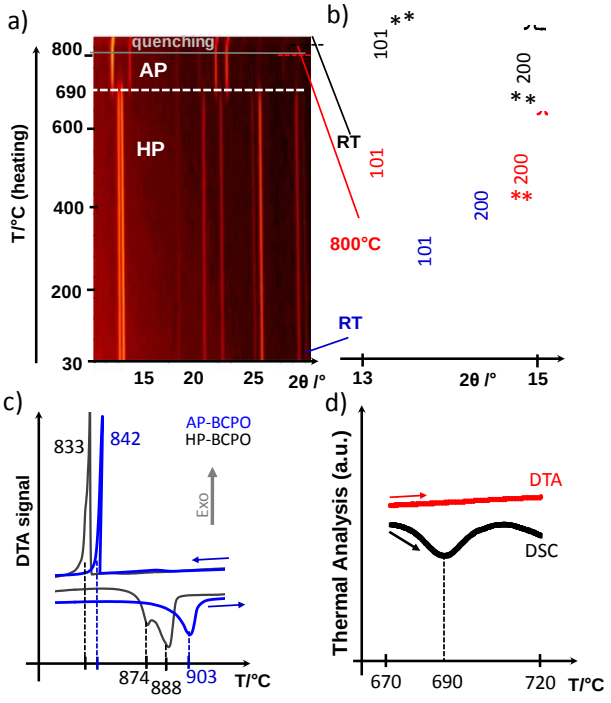


holding the magnetic ladders as structural templates. Finally, the rearrangement between them leads to a scare thermodynamic conjuncture, where both the stable AP and metastable HP forms have nearly the same equilibrium volume and superposed volume dependence of the energy. As a matter of fact, it is responsible for a specific 1st order HP→ AP transition at 690°C in air, observed by DSC but undetected by DTA, likely due to almost unchanged Gibbs energy G, and entropy S= -dG/dT at the HP/AP boundary, see figure 3d. Besides this original phase diagram the achievement of a novel frustrated ladder systems with counter-intuitive hierarchy of magnetic couplings offers a novel playground for exotic magnetic fundamental states.

**Figure 3** : a,b) HT-XRD of HP-BCPO with transition into biphased AP-types at 690°C. c) DTA of the melting and recrystallization of both polymorphs. d) Thermal analyzes of the HP→ AP transformation.

## AUTHOR INFORMATION

***E-mail:** Olivier.mentre@ensc-lille.fr
***E-mail:** altsirlin@gmail.com

## ACKNOWLEDGMENTS

This work was carried out under the framework of the LOVE-ME project supported by the ANR (Grant ANR-16-CE08-0023). The Fonds Européen de Développement Régional (FEDER), CNRS, Région Nord Pas-de-Calais, and Ministère de l'Education Nationale de l'Enseignement Supérieur et de la Recherche are acknowledged for funding the X-ray diffractometers. The authors thank M. legendre at Institut Néel for technical support of the high pressure synthesis.

## REFERENCES

[1] Mentré, O.; Janod, E.; Rabu, P.; Hennion, M.; Leclercq-Hugeux, F.; Kang, J.; Lee, C.; Whangbo, M.-H. ; Petit, S. Incommensurate spin correlation driven by frustration in $BiCu_2PO_6$ *Phys. Rev. B*, **2009**, *80*,180413.

[2] Tsirlin, A. A. ; Rousochatzakis, I.; Kasinathan, D.; Janson, O.; Nath, R.; Weickert, F.; Geibel, C.; Läuchli, A.M. Bridging frustrated-spin-chain and spin-ladder physics: Quasi-one-dimensional magnetism of $BiCu_2PO_6$ *Phys. Rev. B*, **2010**, *82*, 144426.

[3] Mentré, O.; Ketatni, E. M.; Colmont, M.; Huvé, M.; Abraham, F.; and Petricek, V. Structural features of the modulated BiCu2(P(1-x)V(x))O6 solid solution; 4-D treatment of x = 0.87 compound and magnetic spin-gap to gapless transition in new $Cu^{2+}$ two-leg ladder systems *J. Am. Chem. Soc*., **2006**, *128*, 10857–10867.

[4] Alexander, L. K. ; Bobroff, J.; Mahajan, A. V. ; Koteswararao, B.; Laflorencie, N.; and Alet, F. Impurity effects in coupled-ladder $BiCu_2PO_6$ studied by NMR and quantum Monte Carlo simulations. *Phys. Rev. B*, **2010**, *81*, 054438.

[5] Casola, F.; Shiroka, T.; Wang, S.; Conder, K.; Pomjakushina, E.; Mesot, J.; Ott, H.-R. Direct Observation of Impurity-Induced Magnetism in a Spin- 1 2 Antiferromagnetic Heisenberg Two-Leg Spin Ladder *Phys. Rev. Lett.*, **2010**, *105*, 067203.

[6] Casola, F.; Shiroka, T.; Feiguin, A.; Wang, S.; Grbic, M. S.; Horvatic, M.; Krämer, S.; Mukhopadhyay, S.; Conder, K.; Berthier, C.; Ott, H.-R. ; Ronnow, H.M. ; Rüegg, C.; Mesot, J. Field-Induced Quantum Soliton Lattice in a Frustrated Two-Leg Spin- 1/2 Ladder *Phys. Rev. Lett*., **2013**, *110*, 187201.

[7] Choi, K.-Y.; Hwang, J. W.; Lemmens, P.; Wulferding, D.; Shu, G. J.; and Chou, F. C. Evidence for Dimer Crystal Melting in the Frustrated Spin-Ladder System $BiCu_2PO_6$ *Phys. Rev. Lett*., **2013**, *110*, 117204.

[8] Koteswararao, B.; Salunke, S.; Mahajan, A. V.; Dasgupta, I.; and Bobroff, J.; Spin-gap behavior in the two-leg spin-ladder Bi $Cu_2PO_6$ *Phys. Rev. B*, **2007**, *76*, 052402.

[9] Plumb, K. W.; Hwang, K.; Qiu, Y.; Harriger, L.W.; Granroth, G.E.; Kolesnikov, A.I.; Shu, G.J.; Chou, F.C.; Rüegg, C.; Kim, Y.B.; Kim, Y.-J Quasiparticle-continuum level repulsion in a quantum magnet *Nat. Phys*., **2016**, *12*, 224–229.

[10] Jeon, B.-G.; Koteswararao, B.; Park, C. B.; Shu, G. J.; Riggs, S. C.; Moon, E. G.; Chung, S. B.; Chou F. C.; Kim, K. H. Giant suppression of phononic heat transport in a quantum magnet $BiCu_2PO_6$ *Scientific reports*, **2016**, *6*, 36970

[11] Plumb, K. W.; Yamani, Z.; Matsuda, M.; Shu, G.J. ; Koteswararao, B.; Chou, F.C. ; Kim, Y.-J Incommensurate dynamic correlations in the quasi-two-dimensional spin liquid $BiCu_2PO_6$ *Phys. Rev. B*, **2013**, *8*, 024402.

[12] Kohama, Y.; Wang, S.; Uchida, A.; Prsa, K.; Zvyagin, S.; Skourski, Y.; McDonald, R.D.; Balicas, L.; Ronnow, H.M.; Rüegg, C.; Jaime, M. Anisotropic Cascade of Field-Induced Phase Transitions in the Frustrated Spin-Ladder System $BiCu_2PO_6$ *Phys. Rev. Lett.*, **2012**, *109*, 167204.

[13] Kohama, Y.; Mochidzuki, K.; Terashima, T.; Miyata, A.; Demuer, A.; Klein, T.; Marcenat, C.; Dun, Z.L.; Zhou, H.; Li, G.; Balicas, L.; Abe, N.; Matsuda, Y.H.; Takeyama, S.; Matsuo, A.; Kindo, K. Entropy of the quantum soliton lattice and multiple magnetization steps in $BiCu_2PO_6$ *Phys. Rev. B*, **2014**, *90*, 060408.

[14] Nagasawa, H.; Kawamata, T.; Naruse, K.; Ohno, M.; Matsuoka, Y.; Sudo, H.; Hagiya, Y.; Fujita, M.; Sasaki, T.; Koike, Y.; Thermal Conductivity in the Frustrated Two-Leg Spin- Ladder System $BiCu_2PO_6$ *J. Phys. Conf. Ser*., **2014**, *568*, 042012.

[15] Krivovichev, S. V.; Mentré, O.; Siidra, O. I.; Colmont, M. and Filatov, S. K. Anion-Centered Tetrahedra in Inorganic Compounds *Chem. Rev*., **2013**, *113*, 6459–6535.

[16] Abraham, F.; Ketatni, E. M.; Mairesse, G.; and Mernari, B. Crystal structure of a new bismuth copper oxyphosphate: $BiCu_2PO_6$ *Eur. J. Solid State Inorg. Chem*., **1994**, *31*, 313–323.

[17] Radosavljevic, I.; Evans, J. S. and Sleight, A. W. Synthesis and structure of bismuth copper arsenate, $BiCu_2AsO_6$ *J. Alloys Compd*., **1999**, *284*, 99–103.

[18] Whangbo, M.-H.; Koo, H.-J.; and Dai, D. Spin exchange interactions and magnetic structures of extended magnetic solids with localized spins: theoretical descriptions on formal, quantitative and qualitative levels *J. Solid State Chem*., **2003**, *176*, 417–481.

[19] Birch, F. Finite Elastic Strain of Cubic Crystals *Phys. Rev*., **1947**, *71*, 809–824.

[20] Meng, J. F.; Dobal, P. S.; Katiyar, R. S. and Zou, G. T. Optical phonon modes and phase transition in the $Bi_4Ge_{3-x}Ti_xO_{12}$ ceramic system *J. Raman Spectrosc*., **1998**, *29*, 1003–1008.

[21] Arora, A. K.; Yagi, T.; Miyajima, N. and Gopalakrishnan, R. Stability of bismuth orthogermanate at high pressure and high temperature *J. Phys. Condens. Matter*, **2004**, *16*, 8117–8130.

[22] Xiao, W.; Tan, D.; Xiong, X.; Liu, J. and Xu, J. *Proc. Natl. Acad. Sci*., **2010**, *107*, 14026–14029.

[23] Dinnebier, R. E.; Hinrichsen, B.; Lennie, A. and Jansen, M. High-pressure crystal structure of the non-linear optical compound $BiB_3O_6$ from two-dimensional powder diffraction data *Acta Crystallogr. B*, **2009**, *65*, 1–10.

[24] Haussühl, S.; Bohatý, L. and Becker, Piezoelectric and elastic properties of the nonlinear optical material bismuth triborate, $BiB_3O_6$ *P. Appl. Phys. A*, **2006**, *82*, 495–502.

[25] López-de-la-Torre, L.; Friedrich, A.; Juarez-Arellano, E.A.; Winkler, B.; Wilson, D.J.; Bayarjargal, L.; Hanfland, M.; Burianek, M.; Mühlberg, M.; Schneider,

H. High-pressure behavior of the ternary bismuth oxides *J. Solid State Chem.*, **2009**, *182*, 767–777.

[26] Wiehl, L.; Friedrich, A.; Haussühl, E.; Morgenroth, W.; Grzechnik, A.; Friese, K.; Winkler, B.; Refson, K.; Milman, V. Structural compression and vibrational properties of $Bi_{12}SiO_{20}$ sillenite from experiment and theory *J. Phys. Condens. Matter*, **2010**, *22*, 505401.

[27] Henry, N.; Mentre, O.; Boivin, J. C. and Abraham, F. Local Perturbation in $Bi_2CuO_4$ : Hydrothermal Synthesis, Crystal Structure, and Characterization of the New Bi2(Cu1-2xMx)O4 (M = Bi, Pb) *Chem. Mater.*, **2001**, *13*, 543–551.

**Entry for the Table of Contents**

## COMMUNICATION

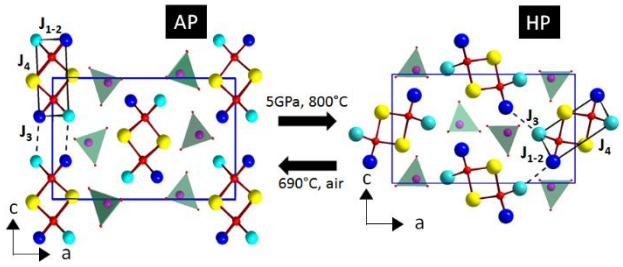


***Marie Colmont, Céline Darie, Alexander A. Tsirlin,* Anton Jesche, Claire Colin, and Olivier Mentré*Page No. – Page No.***

**Compressibility of $BiCu_2PO_6$: polymorphism against S=1/2 magnetic spin ladders**

A metastable high pressure polymorph of $BiCu_2PO_6$ was prepared, with frustrated S=1/2 magnetic ladders similar to those of the ambient-pressure form, but drastically reorganized. It forms an original dual-system with specific relative thermodynamic stability of both forms.